The 15th International Conference on Wind Engineering
Beijing, China; September 1-6, 2019

Temporal response of a bridge deck subject to a wind gust

A. Théodore [a,b], P. Hémon [a], X. Amandolese [a,c]

[a]*LadHyX, Ecole polytechnique-CNRS, Palaiseau, France*
[b]*CTOA-DTecITM, Cerema, Sourdun, France*
[c]*Conservatoire National des Arts et Métiers, Paris, France*

ABSTRACT: Flexible structures such as cable-stayed bridges are subject to dynamic wind loads. These are usually divided into two categories, flutter which is a motion-induced load and buffeting, which is generally considered as an uncoupled load. When these two phenomena are intertwined, it becomes difficult to use spectral methods and time simulation represents a relatively new and better alternative. The present study focuses on a new time-delayed model for the motion-induced pitching moment which can be combined with the effect of a gust. The experimental validation in wind tunnel is provided where flexibly mounted deck sections are submitted to a single gust. Three typical sections, stable or unstable, are considered: the Millau bridge, the Tacoma bridge and the NACA-4412 section.

KEYWORDS: bridge, wind-engineering, temporal simulation, aeroelasticity, flutter, gust

1 INTRODUCTION

Aeroelastic design of bridges have been predominantly conducted in the frequency domain (1). Based on linear formulations of motion-dependent and buffeting loadings, spectral methods are generally sufficient for catching the critical parameters for the onset of flutter or calculating the variance of the dynamical response to a stationary turbulent wind. Nevertheless, spectral methods fail to reproduce neither transient behavior nor nonlinearities. Current challenges in wind engineering are to study nonlinear and transient behavior of structures (2-3), in order to describe effects of highly turbulent winds, or unusual topography effects (4). Because of the mentioned restrictions, these problems can only be solved using a time-dependent framework (5). Time domain analysis of bridge deck response conveniently combine different kinds of wind load including transient gusts effects. It can also take into account structural or aerodynamic nonlinearities (6-7). To account for delayed interaction between fluid and bridges, indicial function generalization can be used (8, 9), or measured (10). On the other hand, Nakamura studied the mechanism of flutter of bluff bodies depending on their aspect ratio and quasi-steady theory (11, 12). He highlighted that fluid memory effects are responsible for the onset of torsional flutter, and that quasi-steady approach generally fails to predict it.

A new and improved version of quasi-steady theory, which includes an additional time-delay component, is introduced. Based on experimental data, this upgraded model should cover fluid memory effects as well. The objective is to propose a time-dependent formulation of pitching moment which is able to reproduce dynamical behavior of a deck under steady and unsteady wind. Such a model has to describe both stable damped behavior and unstable torsional flutter phenomenon. It should also allow the insertion of nonlinearities. The study is restricted to the case of a single degree of freedom bridge deck system (Fig. 4), subject to a gust solicitation, see (Fig. 5), superimposed to steady wind conditions.

Usual wind design procedure requires the results of two different representation of wind forces that are combined to compute both the aeroelastic response to steady wind and the buffeting response of the structure (Fig. 1(a)). It is based on static and dynamic tests in wind tunnel. The alternative approach proposed in this paper (Fig. 1(b)) involves the same kind of wind tunnel tests. It relies on a new formulation of aeroelastic forces where the amplitude is calibrated with static coefficients and on a time-delay computed through the flutter derivatives. Both experimental coefficients are well known to bridge engineering community. Compared to the indicial function approach identified with flutter derivatives that provides the same type of predictions (8, 9), the proposed formulation requires fewer calculations.

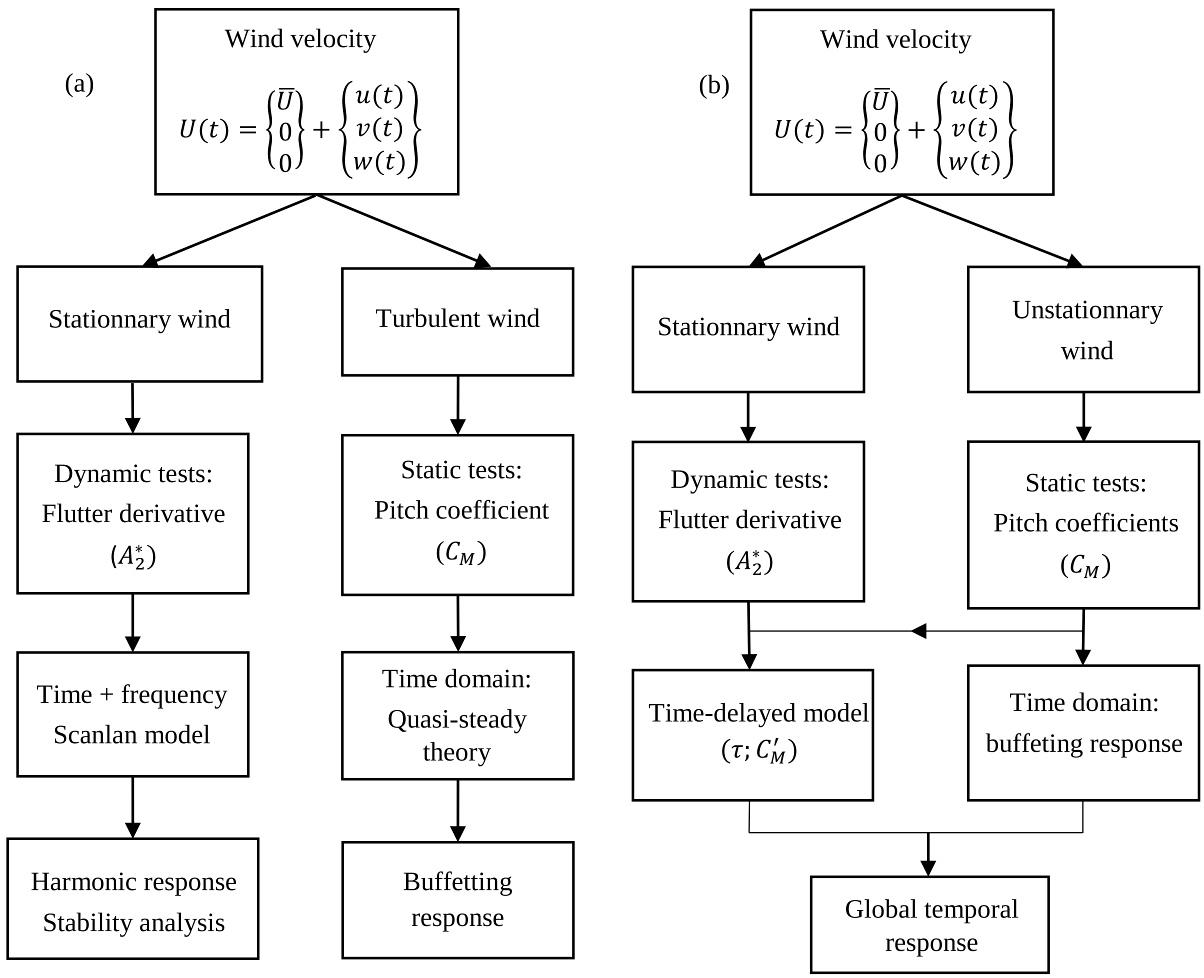

Figure 1 : usual bridges torsion design procedure (a) versus new time-delayed procedure (b)

2 WIND TUNNEL TESTS

2.1 *Structural, aerodynamic and aeroelastic parameters*

Details of the geometry of the cross sections of the model of the Millau viaduct and Tacoma bridge are shown in (Fig. 4). Reduced models are tested in an 18 cm square section wind tunnel. The obstruction coefficient in the vein does not exceed 6% for Millau and 8,5% for Tacoma, for an angle of attack of 10 degrees.

For the static wind tunnel tests, cross-sections are mounted on a force balance. The lift force and the pitching moment are measured for several angles of attack from -12 degrees to +12 degrees (Figs. 3-4). For the dynamic tests, the rigid bridge deck sections are flexibly mounted in pitch.

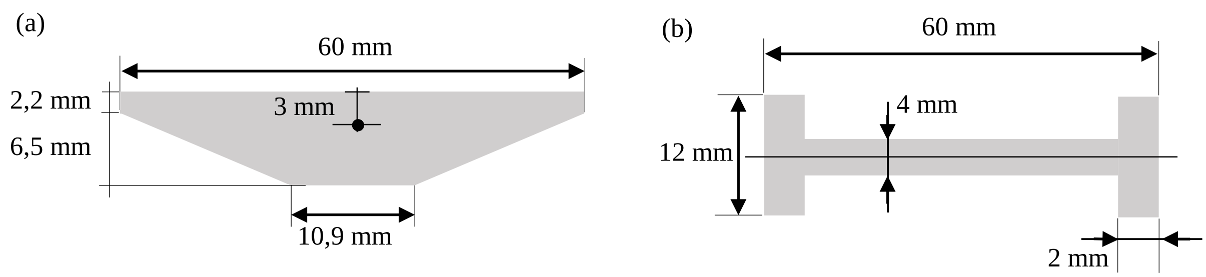

Figure 2 : (a) Millau reduced model scale: 1/460, (b) Tacoma reduced model scale: 1/200

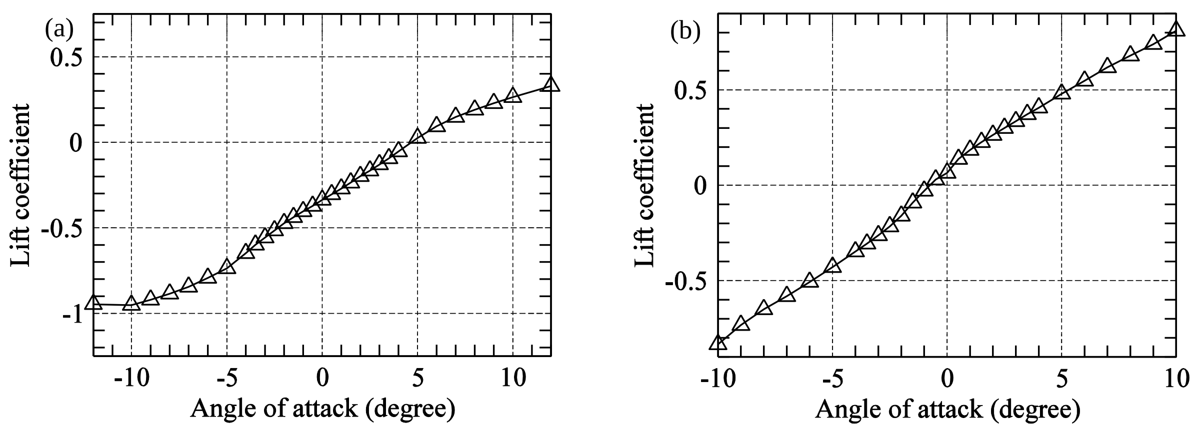

Figure 3 : Static lift coefficient C_z vs angle of attack, (a) Millau Re=78 000, (b) Tacoma Re=70 000

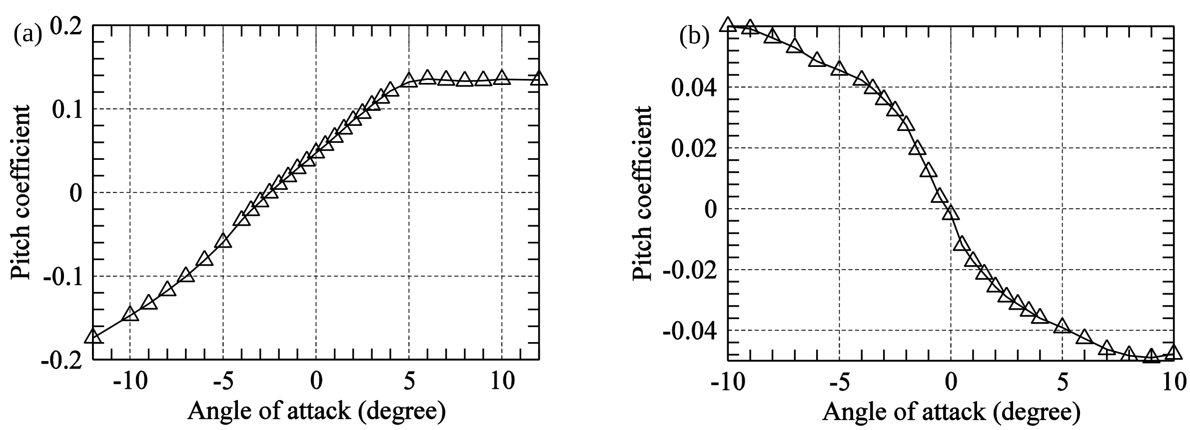

Figure 4 : Static pitch coefficient C_M vs angle of attack, (a) Millau Re=78 000, (b) Tacoma Re=70 000

Table 1 : Millau and Tacoma - slope of static force coefficients

Cross section	Millau	Tacoma
Reynolds number	78 000	70 000
$\boldsymbol{C'_M}$	1,08	-0,86
$\boldsymbol{C'_z}$	3,8	6,15

Table 2 : Dynamic test main parameters

	Natural frequency (Hz)	Structural reduced damping (%)
Millau	11,0	0,12
Tacoma	10,8	1,0

The pitch angle $\theta(t)$ is measured using a laser displacement sensor. Response frequencies of the systems are obtained by spectral analysis. Damping is measured during free decay tests. The structural stiffness k_θ, the reduced damping η_θ and the natural frequency ω_θ are identified without wind (see Table 2). Aerodynamic damping is obtained by subtracting structural damping (small, typically 0.15%) to the total damping measured under wind conditions. Values of flutter derivatives A_2^* versus reduced velocity result from this measurements (Fig. 5).

In order to get the largest consistency of the upcoming results, static and dynamic tests are performed with the same models, in the same wind tunnel, and for the same Reynolds numbers.

The slope of the Tacoma bridge pitching coefficient is negative while it is generally positive for stable structures such as the wings or the Millau viaduct (Table 2). The analysis of bridge flutter stability is generally based on the sign of the flutter derivative A_2^*. However, wind tunnel experiments and results from the literature show that sections with a positive A_2^* generally have a negative C'_M coefficient slope. From this experimental point of view, it seems possible to study the torsional stability of bridge decks, as it is done for some particular bluff body geometries.

2.2 *Experimental and numerical gust simulation*

Gusts are produced in the wind tunnel by a flap mounted upstream (Fig. 6), powered by an engine, so that its motion is perfectly replicable. Within the scope of this study two kinds of gusts with different time length are generated. They are respectively selected to obtain a duration of the perturbation about one period of the system under zero wind condition (case A), and half of this period (case B). The vertical component $w(t)$ of wind speed profile (Fig. 7) measured with hot wires can be fitted using Gaussian functions. Mean values of maximum and minimum amplitudes of vertical components computed from five distinct gust records are plotted versus wind velocity see (Fig. 8).

The simulated transient load due to the gust is written as in (2), using a Küssner's function φ integrated over the non-dimensional time $s = t\,\overline{U}/B$ in (Equ. 2). Duhamel's integral is calculated using the approximation of φ proposed by Jones (13) for an elliptic airfoil (Equ. 3). Note that the longitudinal component of the gust $u(t)$ does not appear in this model.

$$M_y^{gust}(t) = \frac{1}{2}\rho B^2 \overline{U}^2 C_M' \left[\varphi(0)\frac{w(s)}{\overline{U}} + \int_0^s \frac{w(\sigma)}{\overline{U}}\varphi'(s-\sigma)d\sigma\right] \quad (2)$$

$$\varphi(s) = 1 - 0{,}5e^{-0{,}26s} - 0{,}5e^{-2s} \quad (3)$$

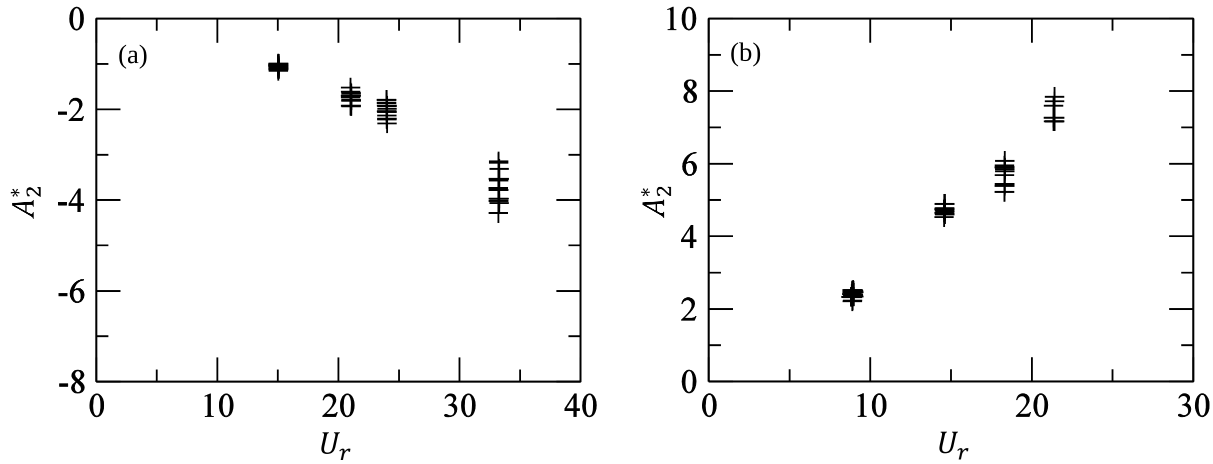

Figure 5: A_2^* flutter derivative vs reduced frequency - Millau (a), Tacoma (b)

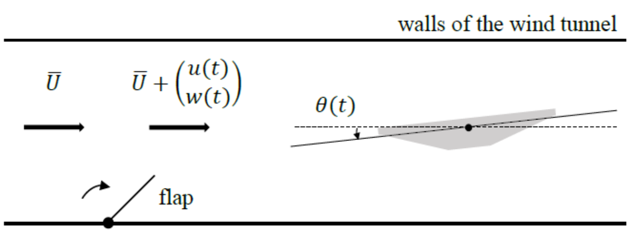

Figure 6 : wind tunnel flap setup

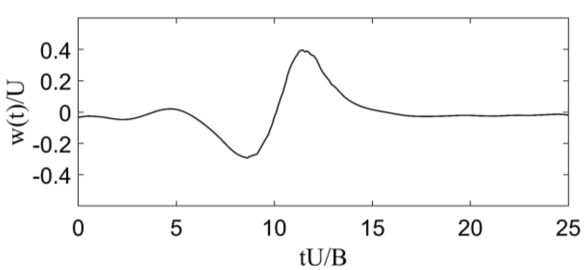

Figure 7: Gust velocity profile vs non-dimensional time

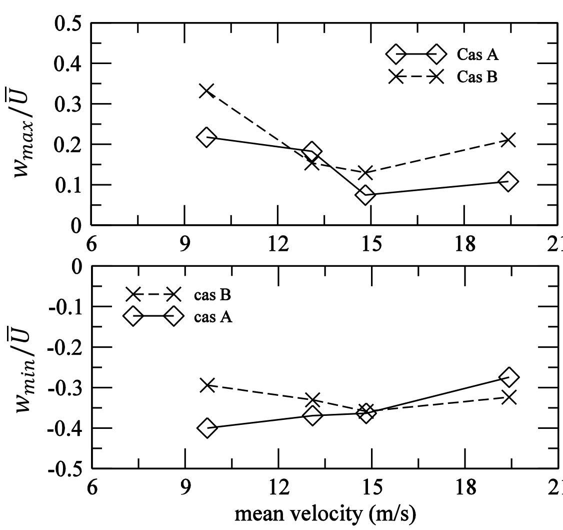

Figure 8: Gust amplitude vs mean velocity

3 NUMERICAL SIMULATION AND VALIDATION

3.1 *Time-delayed pitching moment model*

Quasi-steady approximation neglects fluid memory effects, which are important to predict torsional flutter of bluff bodies (11). Quasi-steady models are based on static aerodynamic coefficients measured in wind tunnel for different position of the bridge decks. They are measured on motionless structures so that the dynamic effect is missing. The time domain model presented here is a simple way to compensate this limit.

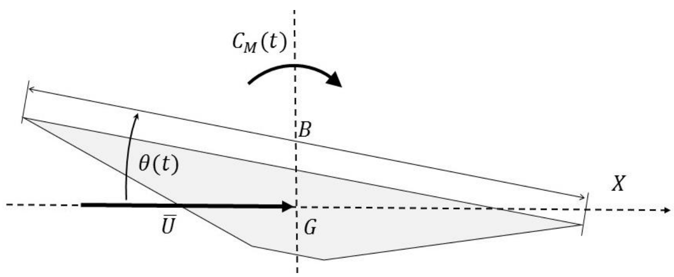

Figure 9: Studied configuration of bridge deck section

The simulated bridge deck section is flexible in pitch. While the rotation axis and gravity center are located at the mid-chord (Fig. 9), the system can be described by the equation of motion:

$$J_0\ddot{\theta} + 2J_0\eta_\theta\omega_\theta\dot{\theta} + k_\theta\theta = M_y^m(t) + M_y^{gust}(t), \tag{4}$$

where $J_0 = k_\theta/\omega_\theta^2$, M_y^m is the motion-induced moment and M_y^{gust} the gust-induced moment.

The motion-dependent load M_y^m is the key of the model. It is formulated thanks to a new time domain model inspired by quasi-steady theory, introducing the time delay τ relative to memory fluid effects (Equ. 5). The lag τ is the time taken by the flow to adapt itself to the new configuration induced by the movement of the bridge. It is similar to previous work achieved in the field of aeroelastic behavior of tube bundles (14) or in-line chimneys (15), where the time delay is introduced to take into account interactions between bodies as in Price & Païdoussis model (16). Delayed aerodynamic behaviors are also used in models of the dynamic stall flutter of airfoils. Leishman and Beddoes (17) developed semi-empirical model for dynamic stall based on a time-delay method where two different time delays are used. One represents the time during which the leading edge vortex process occurs. Stall delay appears in ONERA method as well (18).

$$M_y^m(t) = \frac{\rho\bar{U}^2B^2}{2}C_M(t-\tau). \tag{5}$$

By including the slope of the pitching moment coefficient C_M' at low angle of attack, the motion-induced force can be linearized:

$$M_y^m(t) = \frac{\rho\bar{U}^2B^2}{2}C_M' * \theta(t-\tau). \tag{6}$$

By assuming a periodic motion it is possible to link the time lag with the aerodynamic damping, and so with the so-called flutter derivative A_2^* (1). Introducing $\tau^* = \tau\,\bar{U}/B$ as the non-dimensional time-delay and the reduced velocity $U_r = \bar{U}/fB$ we obtain (Equ. 7):

$$A_2^* = -\frac{C_M'U_r^2}{4\pi^2}\sin\left(\frac{2\pi\tau^*}{U_r}\right). \tag{7}$$

Values of time-delay obtained from (Equ. 7), using A_2^* measured in wind tunnel, are plotted versus U_r in (Fig. 10). Note that in (Equ. 7) the coefficient C_M' is obtained also in wind tunnel by static tests. It is positive for the stable streamlined sections, Millau and NACA and negative for the Tacoma unstable section. An important result of (Fig. 10) is that the condition $\tau^*/U_r < ½$ remains valid, so that the sign of A_2^* is completely imposed by the sign of C_M'. This result is similar to the stability criterion established by Nakamura [11] on small aspect ratio bluff bodies.

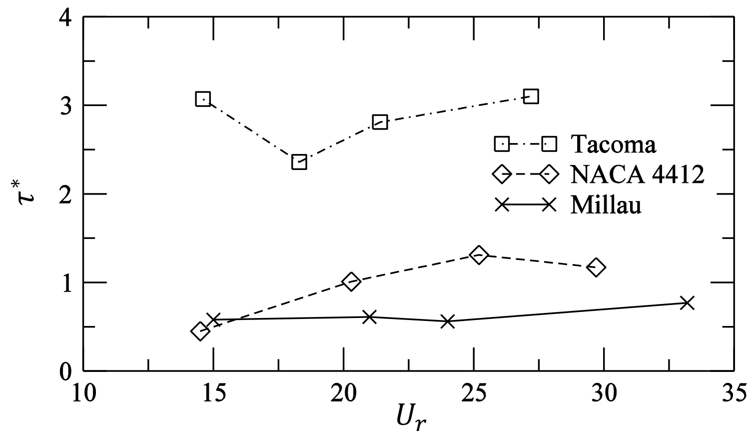

Figure 10: Non-dimensional time delay $\boldsymbol{\tau}^*$ vs reduced velocity $\boldsymbol{U_r}$

3.2 *Physical interpretations of the time-delay parameter*

Physically, the values of τ^* are connected with the adaptation delay of the flow to the bridge's motion. This may explain why, it is found that streamlined cross-sections (e.g. Millau or NACA) are characterized by smaller values of τ^* than bluff bodies (e.g. Tacoma) for which stalled flow is much more dominant.

Let $B/\overline{U} = T_{wind}$ be the fluid's characteristic time, required by a particle of fluid to travel across the bridge deck section. Then $\tau^* = \tau/T_{wind}$ is the ratio between the time-delay and the fluid travel time. It represents a time scale of the flow disturbances due to the obstacle. For the Millau deck, τ^* is lower than one, indicating that the time-delay is smaller than the fluid travel time. On the contrary, for the Tacoma bridge τ^* is about three, indicating that the time-delay is much greater than the fluid travel time. Observations show that unstable sections are characterized by time-delays longer than the fluid travel time, whereas the time-delays of stable sections are of the order of magnitude or smaller than the fluid travel time. But in either case, it is experimentally demonstrated that the variations of τ^* remain without influence on the flutter stability of the bridge decks, which is controlled only by the sign of C_M'.

The time delay τ^* can also be seen as a portion of the reduced velocity. If it is between zero and $U_r/2$, system is stable if $C_M' > 0$, and unstable if $C_M' < 0$. If it is between $U_r/2$ and U_r, system is unstable if $C_M' > 0$, and stable if $C_M' < 0$. Recall however that bridge decks belong to the first category.

Furthermore one can observe (Fig. 10) that some results obtained with Tacoma reduced model are close to the maximum value of aerodynamic damping which can be estimated trough the proposed time-delay model, which is reached when $\tau^* = \tau_{lim}^* = U_r/4$. Indeed, when $U_r = 14.6$ then $\tau_{lim}^* = 3.65$, just larger than the value shown in (Fig. 10). The highest value (either positive or negative) of the corresponding flutter derivative is then $A_{2_{limit}}^* = -C_M' U_r^2/4\pi^2$. This is consitent with the fact that H-shape cross sections are known for having higher negative aerodynamic damping than other current bridge sections (1). Thus, despite this limitation, the time-delay model should be able to predict torsionnal behavior of most existing bridges, which are usually better profiled.

3.4 *Results and comparison with wind tunnel tests*

Finally, simulation of pitching motion is plotted simultaneously with the corresponding records of measurements in wind tunnel. Response accounts for both terms, movement and gust induced loads according to (Equ. 4). An example of simulated and measured motions of the Millau cross-section, subject to a gust excitation, is presented in (Fig. 11). Both transient and steady-state results are in good agreement with experiments. Indeed, amplitude of initial bump and damped decay are computed with a good accuracy.

Another example of simulated motion with the unstable cross-section of the Tacoma bridge subject to motion-dependent wind loads only is shown in (Fig. 12). Here the instability is triggered by residual wind tunnel turbulences after a short time. The behaviour at small angles of attack is in good agreement with the experiments. The differences appear at higher angles of attack, especially above 5 degrees, due to aerodynamic non-linearities. It may be noted that the implementation of a non-linear expression of the pitching coefficient in the model, instead of the linearized (Equ. 6), could significantly improve the simulation at larger amplitude of motion.

4 CONCLUSIONS

A new time delay approach of motion-induced forces shows good ability to calculate the torsional behavior of bridge decks subjected to a single gust versus time. The model requires classical experimental results already used in wind engineering, such as the static force coefficients and the flutter derivative A_2^*. A link between the non-dimensional time delay of the pitching moment is established with the aerodynamic damping, providing a physical meaning consistent with experimental results. Moreover, identification of a range of reduced velocity in which the time-delay is almost constant for a given deck cross-section seems possible. Direct relationship between the slope of pitch coefficient and the flutter stability is also established. This provides a useful design tool to the structural engineering community. The variance and the extreme values of the buffeting response of bridge decks are explored in an additional work which compares experimental results and time simulations.

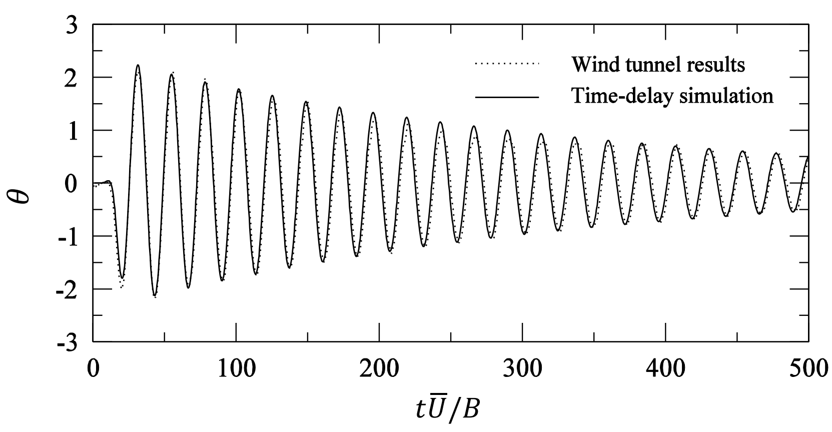

Figure 11: Response to a single gust versus non-dimensional time – Millau deck, gust case A, $U_r = 21$

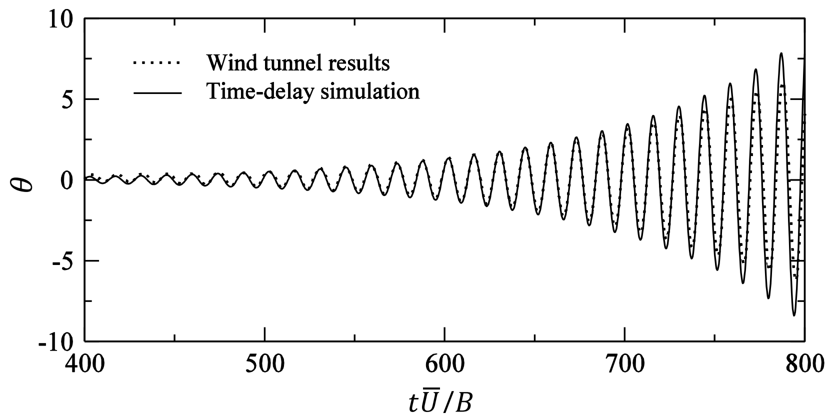

Figure 12: Response to steady wind versus non-dimensional time – Tacoma deck, $U_r = 14{,}6$

5 REFERENCES

1 R.H. Scanlan, J.J. Tomko, Airfoil and bridge deck flutter derivatives, J. Eng. Mech. Div., ASCE(1971) 1717-1737.
2 X. Amandolese, et al., The transient temporal response of a flexible bridge deck subjected to a single gust, J. of Comp. App. Math. 246 (2013) 153-160.
3 S. Manzoor, et al., On the aeroelastic transient behavior of a streamlined bridge deck section in a wind tunnel, J. Fluids Struct. 27 (2011) 1216-1227.
4 A.G. Davenport, Vulnerability of long span bridges to wind, IABSE congress report volume 15 (1996) 1031-1042.
5 X. Chen, A. Kareem, Aerodynamic analysis of bridges: effects of turbulence and aerodynamic nonlinearities, J. Eng. Mech. (2003) 885-895.
6 G. Diana et al., New numerical approach to reproduce bridge aerodynamic non-linearities in time domain, J. of Wind Engineering and Industrial Aerodynamics 96 (2008) 1871-1884.
7 H.Y. Farsani et al., Indicial functions in the aeroelasticity of bridge decks, J. Fluids Struct 48 (2014) 203-215.
8 X. Chen, et al., Time domain flutter and buffeting response analysis of bridges, J. Eng. Mech, (2000) 7-16.
9 L. Caracoglia, NP. Jones, Time domain vs. frequency domain characterization of aeroelastic forces for bridge deck sections, J. of Wind Engineering and Industrial Aerodynamics 91 (2003) 371-402.
10 S. Miranda et al., Indicial function and flutter derivative: a generalized approach of the motion related wind loads, J. Fluids Struct 42 (2013) 466-487.
11 Y. Nakamura, T. Mizota, Torsional flutter of rectangle prisms, J. Eng. Mech. 101 (1975) 125-142.
12 Y. Nakamura, On the aerodynamic mechanism of torsional flutter of bluff structures, J. of Sound and Vibration 67 (1979) 163-177.
13 Y.C. Fung, An introduction to the Theory of aeroelasticity, Dover, New York, 1993.
14 P. Hémon, An improvement of the time delayed quasi-steady model for the oscillations of circular cylinders in cross-flow, J. Fluids Struct. 13 (1999) 291-307.
15 M-T. Bourdeix, et al., Wind induced vibrations of chimneys using an improved quasi-steady theory for galloping, J. of Wind Engineering and Industrial Aerodynamics 74-76 (1998) 785-794.
16 S. J. Price, M. P. Païdoussis, An improved mathematical model for the stability of cylinder rows subject to cross flow, J. of Sound and Vibration 97 (1984) 615-640.
17 J. G. Leishman, T. S. Beddoes, A semi-empirical model for dynamic stall, J. of the American Helicopter Soc. 34 (1989) 18-29.
18 K. W. McAlister et al., Application of the ONERA model of dynamic stall, NASA technical paper 2399 (1984), report 84-A-3.